Accepted Manuscript

Dual-targeting Rutaecarpine-NO donor hybrids as novel anti-hypertensive agents by promoting release of CGRP

Jinjin Ma, Lan Chen, Jinbao Fan, Wei Cao, Guangyao Zeng, Yajing Wang, Yuanjian Li, Yingjun Zhou, Xu Deng

PII: S0223-5234(19)30151-5

DOI: https://doi.org/10.1016/j.ejmech.2019.02.037

Reference: EJMECH 11129

To appear in: *European Journal of Medicinal Chemistry*

Received Date: 17 November 2018

Revised Date: 23 January 2019

Accepted Date: 10 February 2019

Please cite this article as: J. Ma, L. Chen, J. Fan, W. Cao, G. Zeng, Y. Wang, Y. Li, Y. Zhou, X. Deng, Dual-targeting Rutaecarpine-NO donor hybrids as novel anti-hypertensive agents by promoting release of CGRP, *European Journal of Medicinal Chemistry* (2019), doi: https://doi.org/10.1016/j.ejmech.2019.02.037.

Graphic Abstract

Dual-targeting Rutaecarpine-NO Donor Hybrids as Novel Anti-hypertensive Agents by Promoting Release of CGRP

Jinjin Ma,[†,1] Lan Chen,[†,1] Jinbao Fan,[†] Wei Cao,[†] Guangyao Zeng,[†] Yajing Wang,[‡] Yuanjian Li,[†] Yingjun Zhou,[*,†] Xu Deng[*,†]

A series of rutaecarpine-NO donor hybrids were designed, synthesized and evaluated. Among which, **13a** exhibited significantly improved vasodilator activity, which is probably effected via synergistically activating TRPV1 and TRPA1 to promoting the release of CGRP.

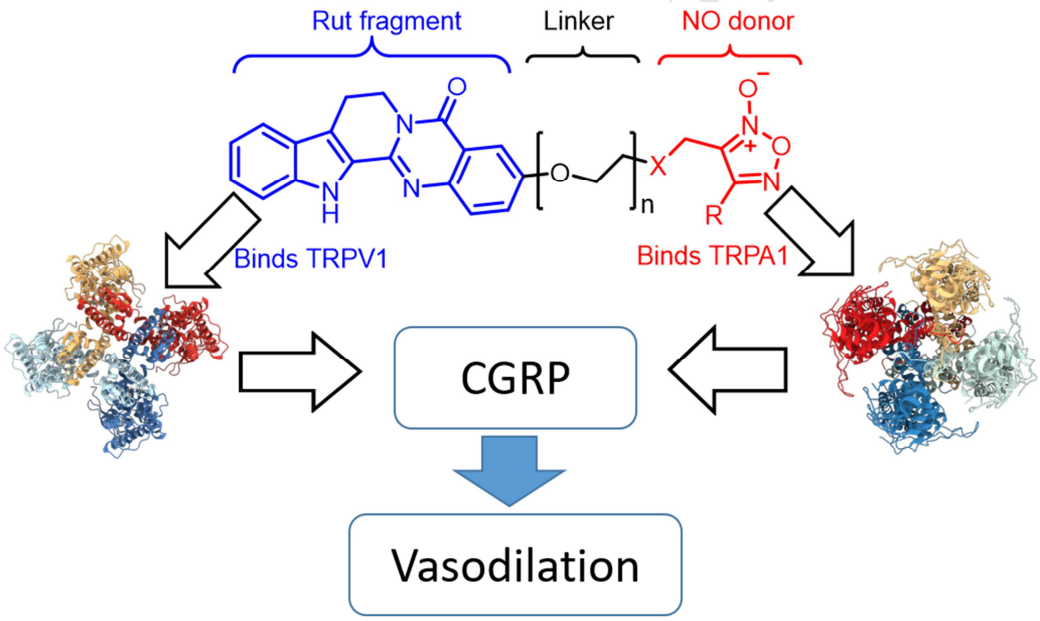

Dual-targeting Rutaecarpine-NO Donor Hybrids as Novel Anti-hypertensive Agents by Promoting Release of CGRP

Jinjin Ma,[†,‡] Lan Chen,[†,‡] Jinbao Fan,[†] Wei Cao,[†] Guangyao Zeng,[†] Yajing Wang,[‡] Yuanjian Li,[†] Yingjun Zhou,[*,†] Xu Deng[*,†]

[†]Xiangya School of Pharmaceutical Science, Central South University, Changsha 410013, Hunan, China

[‡]Hunan University of Chinese Medicine, Changsha, 410028, Hunan, China

*E-mail: dengxu3817@csu.edu.cn, zhouyingjun@csu.edu.cn

[‡]These authors contribute equally to this work.

Abstract:

CGRP, known as the most potent vasodilator substance, plays an important role in hypertension initiation and development. TRPV1 and TRPA1 are critical in promoting the synthesis and release of CGRP, thereby regulating the cardiovascular tone. Rutaecarpine exhibits potent vasodilator and hypertensive effects by stimulating CGRP synthesis and release via activation of TRPV1. And NO has been shown to react with H_2S *in vivo* to form HNO, thereby activating HNO-TRPA1-CGRP pathway. Inspired by combination therapy, 11 rutaecarpine-furoxan hybrids were designed, synthesized and evaluated. The results demonstrated that most hybrids exerted comparable or improved vasodilator activities. Among which, **13a** is the most potent both *ex vivo* (EC_{50} = 13.1 nM) and *in vivo*. Mechanistic studies revealed that the vasodilator and anti-hypertensive effects of the hybrids might involve the promotion of CGRP release via dual activation of TRPV1 and TRPA1. This work suggests that dual-targeted hybrids might be an effective and promising approach to discover and develop novel anti-hypertensive drugs.

Keywords: CGRP, dual-targeting, rutaecarpine-NO donor hybrids, anti-hypertensive agents

1. Introduction

Hypertension is one of the leading risk factors for many disease conditions, including stroke, hypertensive heart disease, coronary artery disease, kidney disease, and aneurysms[1]. Approximately 177 million people in china are estimated to be living with hypertension, with low rates of awareness and control of this condition[2]. Despite wide array of effective and in-expensive anti-hypertensive treatments are available, the disease remains uncontrolled in nearly 50% of affected patients. Furthermore, the number of patients with resistant hypertension continues to increase. Most of clinically available anti-hypertensive agents can not be used as a single drug therapy because of several toxicities, side effects associated with these drugs. Multiple dose therapies make the regime complicated and less successful. Therefore, a combination drug therapy by designing drugs with more than one active pharmacophores in one molecule, namely hybrid molecule, is promising.

Calcitonin gene-related peptide (CGRP), also known as the most potent vasodilator neuropeptide in capsaicin-sensitive sensory nerves, is widely distributed in cardiovascular system[3]. Plasma levels of CGRP are significantly decreased in patients with essential hypertension and in spontaneously hypertensive rat (SHR)[4, 5]. Moreover, CGRP plays an important role in mediating cardiovascular protection against damages to multiple tissues, such as ischaemia-reperfusion (I/R) injury and endothelium impairment[6]. Therefore, regulating the synthesis and release of CGRP represents a new approach to novel anti-hypertensive drug discovery.

Transient receptor potential vanilloid 1 (TRPV1), a polymodal nonselective cation channel, is a key receptor in regulation of the CGRP synthesis and release[7]. Activation of the TRPV1 expressed in sensory nerves leads to the release of endogenous vasodilators, including CGRP and substance P[8]. TRPV1 is also involved in Dahl salt-sensitive hypertension[9]. Besides, transient receptor potential channel ankyrin 1 (TRPA1) also plays a key role in regulation of CGRP synthesis and release [10-12]. TRPA1 is expressed in small to medium diameter neurons which predominately co-express TRPV1[13]. Cinnamaldehyde, isothiocyanates and some noxious compounds can activate TRPA1 by covalent modification of cysteine[14],

thereby leading to vasodilator effect. The effect of can be eliminated in TRPA1 knockout mice[11]. Taken together, both TRPV1 and TRPA1 are promising therapeutic targets for anti-hypertensive drug discovery and development[15].

Rutaecarpine (**Rut**), a quinazolinocarboline-type alkaloid, is a major bioactive constituent in *Evodiae Fructus*, which has been prescribed for treatment of hypertension in traditional Chinese medicine[16-18]. Studies demonstrated that rutaecarpine exerts vasodilator[19], positive inotropic[20] and chronotropic and myocardium-protective effects[21] via stimulation of CGRP synthesis and release by activation of TRPV1. However, the poor water solubility and bioavailability, as well as the immune-mediated toxicity and acute toxicity, have precluded it as new anti-hypertensive agent[22, 23]. Though several structure modifications and SARs studies have been reported[24], no derivatives with significantly improved vasodilator activity and bioavailability have been reported as far as our knowledge. Thus there is an urgent need to develop a new strategy to modify rutaecarpine.

[Insert Figure 1 Here]

Nitric oxide (NO) is a well-known vasodilator in cardiovasocular system[25]. It plays a key role in hypertension initiation and development[26]. Recently, Filipovic revealed that NO-evoked vasodilatatory effects largely through reacting with H_2S *in vivo* to form HNO, thereby activating HNO-TRPA1-CGRP pathway [27-29].

Because of the crosstalks between **Rut** and NO donors by stimulating CGRP, adjunctive **Rut**-NO donors should be a promising means for improving vasodilator activity and safty of the anti-hypertensive drug. Moreover, this hybrid approach may do good to gain tissue-specific NO related function, since NO is a dispersive gas messenger that can elicit a variety of biological acitivities. On the other hand, furoxans are thermally stable and represent a optimal class of NO donors that can produce high levels of NO, thereby eliciting a variety of biological activities *in vivo*[30]. Herein, we present the design and synthesis of novel **Rut**-NO donor hybrids as potent vasodilators, which is probably effected by dually activating TRPV1 and TPRA1 to promote the release of CGRP.

2. Results and Discussion

2.1. Chemistry

2.1.1. Synthesis of rutaecarpine derivatives

Since A-ring and E-ring substituents exert limited impact on the vasodilator activity according to Hu's results[24], our design and synthesis of rutaecarpine derivatives were focused on the A-ring and E-ring in order to maintain the vasodilator activity of the framework.

The synthesis of rutaecarpine framework follows the procedures developed by Su[31]. As is illustrated in scheme 1, the synthesis commenced with protection of the pendant Nb of tryptamines **1a-1b** with formyl group by ester-amine exchange with ethyl formate, which afforded formyl amide **2a-2b** quantitively. Subsequent $POCl_3$ mediated intramolecular Pictet-Spengler reaction gave the *β*-carboline intermediates **3a-3b** in excellent yields. As reported in the literature[31], the rutaecarpine derivaties **5a-5c** were facilitated via carboiimide-mediated condensation of **3a-3b** with anthranilic acid **4**.

[Insert Scheme 1 Here]

2.1.2. Synthesis of furoxans and linkers

The synthesis of furoxan-type NO donors was illustrated in Scheme 2a. One-pot condensation/decarboxylation sequence of **6a-6g** with malonic acid in the presence of piperidine delivered α,β-unsaturated acids **7a-7g** in good yields, which was selectively reduced to allylic alcohols **8a-8g** by BH_3-THF. Subsequently, [3+2] dipolar reaction of **8a-8g** with $NaNO_2$ in AcOH, followed by activation of alcohol with Ms group to afford the desired furoxans **9a-9g** in moderate to good yields.

As shown in Scheme 2b, the linkers **11a** and **11b** were prepared starting from polyethylene glycol by activation with methanesulfonyl chloride, followed by substituting with NaN_3.

[Insert Scheme 2 Here]

2.1.3. Synthesis of rutaecarpine-furoxan hybrids

With rutaecarpine derivatives and furoxan-type NO donors in hand, we then turned to combine two fragments together with PEG linker. For E-ring modified rutaecarpine-furoxan hybrids, the Ms-activated PEG linkers **11a** and **11b** were first

attached to the C3-OH of rutaecarpine derivative **5b** to form ether, followed by catalytic reduction to afford amine intermediates **12a** and **12b** in good yields. Subsequently, alkylative coupling of **12** and furoxans delivered the desired rutaecarpine-furoxan hybrids **13a-13i** in moderate yields.

For A-ring modified rutaecarpine-furoxan hybrids, a modified procedure was developed. As shown in Scheme 2, rutaecarpine derivative **5a** was first demethylated by treatment of BBr_3 to afford **14** in good yield. However, direct installation of PEG linker at C-10 position furnishing the desired product **15** in low yield, which is presumably due to the contaminated side reaction of N-13 with the PEG linker. Subsequently, **15** was coupled with furoxan **9a** following the procedure described above, thereby giving the A-ring modified rutaecarpine-furoxan hybrid **16** in good yield.

Besides, N13-modified rutaecarpine-furoxan hybrid was prepared following the routine procedures. Starting from rutaecarpine, alkylation at N-13 position in the presence of NaH, followed by catalytic reduction and alkylation at the pandent amine group, gave the intermediate **17** and the N13-modified rutaecarpine-furoxan hybrid **18** successively.

[Insert Scheme 3 Here]

2.2. Biological Results and Discussion

With a diverse set of rutaecarpine-furoxan hybrids in hand, we next evaluated their vasodilator activities by the rat aortic ring assay with rutaecarpine as the positive control. As shown in figure 2 and table 1, the vasodilator effects in different concentrations were measured and the EC50 were calculated, respectively.

Based on the biological results, the structure-activity relationships of rutaecarpine-furoxan hybrids were discussed. Generally, **13a** and **13i** exhibited significant improved vasodilator activity over the parent compound rutaecarpine, and **13b**, **13c**, **13d**, **13h, 16** and **18** showed comparable activity to that of rutaecarpine, while **13e**, **13f**, **13g** were less potent. In-depth investigations revealed that a variety of structure features exerted impacts on the biological profile, including the aryl

substituents on the furoxan moiety, the length of the linker, the coupling position on the rutaecarpine backbone. We would like to discuss the factors as follows.

In term of aryl substituens on the furoxan moiety, it seems that electron withdrawing groups are benificial to the vasodilator effects (see **13c**, **13d** and **13h**), whereas electron donating ones are not (see **13b**, **13e**, **13f** and **13g**). This may attribute to the reason that electron withdrawing substituents, but not electron donating ones, facilitate the release of NO from the furoxan moiety, thereby producing enhanced vasodilator activity. For the length of the linker, it is obvious that the shorter the linker, the better the vasodilator activity (see **13a** *vs* **13b** and **13i**). Besides, the position that the furoxan fragment attaches to the rutaecarpine also exerts significant impacts on the activities. Specifically, 3-position and 10-position (see **13b** and **16**) are optimal than 13-positions (see **18**). This means substituents at A-ring and E-ring exert less impact on the activities than that at B-ring, which is in consistent with that in Hu's work[24]. These results will also provide guidelines for our further investigations.

To prove whether the hybrid strategy is optimal than simple combination strateggy, we also performed a control experiment. As shown in figure 2 and table 1, the vasodilator activity of **13a** is more potent than that of the group by simple combination of **Rut** and furoxan at 1:1 ratio, which indicates that the hybrid strategy is superior.

[Insert Figure 2 and Table 1 Here]

To elucidate whether the rutaecarpine-furoxan hybrids evoke vasodilator effects by activating TRPA1 and TRPV1 to promote the release of CGRP, several control experiments were performed with **13a** as a model compound. The rat aortic rings were co-incubated with **13a**, L-cysteine and the competitive TRPV1 antagonist capsazepine, or the competitive TRPA1 antagonist HC030031, or selective CGRP receptor antagonist CGRP-(8-37) at a diverse set of concentrations, and the vasodilator effects were recorded. As illustrated in figure 3, the vasodilator effects of **13a** can be significantly eliminated by TRPV1 antagonist, or TRPA1 antagonist, or both of them, or CGRP antagonist. These results suggest that rutaecarpine-furoxan hybrid **13a**

probably exerts its vasodilator activity by activating TRPA1 and TRPV1 to stimulate the release of CGRP.

[Insert Figure 3 Here]

Furthermore, we also evaluated the *in vivo* blood pressure lowering effects of **13a** with SD rat. It is revealed that **13a** could significantly lower the systolic and diastolic pressure at both low (20 mg/kg) and high (40 mg/kg) dosages. Comparing to the rutaecarpine group, the systolic pressure lowering effect of **13a** is more significant than that of rutaecarpine at both low and high dosages. Whereas, the diastolic pressure lowering effect of **13a** is more significant than that of rutaecarpine only at high dosage. However, when we tried to measure the CGRP level in the blood between **13a**-treatment group and **Rut**-treatment group with ELISA assay, it turned out to be no difference (see Figure S1). This might attribute to the low sensitivity of ELISA method and the relatively low CGRP level in the blood of rats.

[Insert Figure 4 Here]

3. Conclusion

In summary, we have designed and synthesized a series of rutaecarpine-furoxan hybrids as novel anti-hypertensive agents. As mentioned above, the structure-activity relationship studies of these hybrids were discussed and most hybrids exerted more potent or comparable vasodilator effect than rutaecarpine in rat aortic ring assay. Using **13a** as a model compound, the functional investigations revealed that the vasodilator and anti-hypertensive effects of these hybrids might involve the promotion of CGRP release via dual activation of TRPV1 and TRPA1. This work demonstrates that the design of hybrids that dually targeting TRPV1 and TRPA1 might be an effective and promising approach for novel anti-hypertensive drug discovery and development. However, the detailed mechanism responsible for the vasodilator and anti-hypertensive effects of the hybrids still requires further investigations. The molecular pharmacological studies to find direct evidence of activating TRPV1 and TRPV1 are underway.

4.1. Experimental Section

4.1. Chemistry

4.1.1. General information

All reagents were commercially available and used without further purification unless indicated otherwise. CH_3CN, DCM, DMF were distilled over CaH_2. Thin layer chromatographies were carried out on GF254 plates (0.25 mm layer thickness). Flash chromatography was performed with 300–400 mesh silica gels. Visualization of the developed chromatogram was performed by fluorescence quenching or by ceric ammonium molybdate, or $KMnO_4$ stain. Yields reported were for isolated, spectroscopically pure compounds.

^1H and ^{13}C–NMR experiments were performed on a Bruker AM-400 and AM-500 NMR spectrometer at ambient temperature. The residual solvent protons (^1H) or the solvent carbons (^{13}C) were used as internal standards. ^1H-NMR data are presented as follows: chemical shift in ppm downfield from tetramethylsilane (multiplicity, coupling constant, integration). The following abbreviations are used in reporting NMR data: s, singlet; br s, broad singlet; d, doublet; t, triplet; q, quartet; qt, quartet of triplets; dd, doublet of doublets; dt, doublet of triplets; AB, AB quartet; m, multiplet. ESI-MS were recorded with a Mariner mass spectrometer and HRESIMS on an Agilent Technologies LC/MSD TOF instrument. Individual compounds with a purity of > 95% were used for biological experiments.

*4.1.2. Procedures for the preparation of compounds **5a-5c**, **9a-9g**, **11** and **14** are illustrated in Supplementary Information (SI).*

4.1.3. Procedures for the preparation of 3-(((5-oxo-5,7,8,13-tetrahydroindolo[2',3':3,4] pyrido[2,1-b]quinazolin-3- yl)oxy)methyl)-4-phenyl-1,2,5-oxadiazole-2-oxide (**13a**)**.**

To a solution of **5b** (60 mg, 0.2 mmol) and **9a** (54 mg, 0.2 mmol) in MeCN was added K_2CO_3 (41 mg, 0.3 mmol), the resulting mixture was stirred at 80 °C until no starting material was detected by TLC. The reaction was quenched with H_2O (30 mL) and extracted with EtOAc (50 mL × 3). The combined organic layer was washed brine, dried with anhydrous Na_2SO_4, and concentrated in vacuum. The crude product was purified by silica gel column chromatography (pure DCM) to afford **13a** as a yellow

solid (59 mg, 62%). **^{1}H-NMR** (500 MHz, DMSO-d_6): δ 11.83 (s, 1H), 7.85 (dd, *J* = 8.1, 1.5 Hz, 2H), 7.70 (d, *J* = 3.0 Hz, 1H), 7.68 – 7.57 (m, 5H), 7.48 (d, *J* = 8.3 Hz, 1H), 7.44 (dd, *J* = 8.9, 3.0 Hz, 1H), 7.26 (t, *J* = 11.7, 1H), 7.09 (t, *J* = 7.5 Hz, 1H), 5.37 (s, 2H), 4.45 (t, *J* = 6.9 Hz, 2H), 3.18 (t, *J* = 6.9 Hz, 2H); **^{13}C-NMR** (126 MHz, DMSO-d_6) δ 160.6, 157.6, 155.4, 144.5, 143.3, 139.1, 132.0, 129.9, 128.9, 128.1, 127.6, 126.1, 125.4, 125.1, 124.7, 121.9, 120.3, 120.2, 117.8, 113.0, 112.9, 109.5, 59.6, 41.5, 19.4; **HR-ESI-MS** (*m/z*): calcd. for $C_{27}H_{20}N_5O_4$ $[M+H]^+$, 478.1510, found 478.1508.

4.1.4. General procedure for the preparation of rutaecarpine-furoxan hybrids ***13b~13i***

Step 1: To a solution of **5b** (1.51 g, 5 mmol) and **11** (1.27 g, 5 mmol) in DMF was added K_2CO_3 (1.04 g, 7.5 mmol), the mixture was stirred at 80 °C overnight. Then the solvent was removed by a rotary evaporator, the residue was extracted with DCM (80 mL × 3), the combined organic layer was washed with brine and dried over anhydrous sodium sulfate, filtered, and concentrated by a rotary evaporator, the resulting crude product was purified by silica gel column chromatography (DCM : MeOH = 150 : 1) to afford 3-(2-(2-(2-azidoethoxy)ethoxy)ethoxy)-7,8-dihydroindolo [2',3':3,4]pyrido [2,1-*b*]quinazolin-5(13*H*)-one as a yellow solid (1.89 g, 82 %).

The product above (1.89 g, 4.1 mmol) and Pd/C (189 mg, 10%wt) was suspended in methanol (50 mL) under H_2 (1 atm). The resulting mixture was stirred at room temperature vigorously until no starting material was detected by TLC. Then the suspension was filtered and the filtrate was concentrated in vacuum. The residue was purified by flash column chromatography (DCM: MeOH = 10:1 to 5:1) to afford **12** as a yellow solid (1.19 g, 67%).

Step 2: To a solution of **12** (87 mg, 0.2 mmol) in CH_3CN (2 mL) was added compound **9b-9g** (0.2 mmol), the resulting mixture was stirred at 60 °C for 6 h. Then the solvent was removed in vacuum. The residue was purified by flash column chromatography (DCM : MeOH = 150 : 1) to obtain rutaecarpine-NO donor hybrids **13b~13h** in 55 % to 67 % yields.

4.1.4.1. 3-(((2-(2-(2-((Rutaecarpin-3-yl)oxy)ethoxy)ethoxy)ethyl)amino)methyl)-4-phenyl-1,2,5-oxadiazole-2-oxide (**13b**)

Yield: 58%, yellow solid. **^{1}H-NMR** (500 M Hz, DMSO-d_6): δ 11.82 (s, 1H), 7.98 – 7.88 (m, 2H), 7.67 – 7.52 (m, 6H), 7.48 (dd, *J* = 8.2, 2.4 Hz, 1H), 7.40 (dt, *J* = 8.8, 3.1 Hz, 1H), 7.30 – 7.21 (m, 1H), 7.08 (td, *J* = 7.9, 2.9 Hz, 1H), 4.44 (dd, *J* = 6.6, 3.6 Hz, 2H), 4.17 (d, *J* = 2.1 Hz, 2H), 3.81 (d, *J* = 3.1 Hz, 2H), 3.76 (d, *J* = 1.8 Hz, 2H), 3.60 – 3.55 (m, 2H), 3.50 (d, *J* = 4.7 Hz, 2H), 3.44 (d, *J* = 3.3 Hz, 2H), 3.16 (dd, *J* = 6.4, 3.7 Hz, 2H), 2.65 (d, *J* = 3.2 Hz, 2H); **^{13}C-NMR** (126 MHz, DMSO-d_6): *δ* 160.8, 157.8, 157.0, 143.8, 142.2, 139.0, 131.6, 129.6, 128.6, 128.3, 127.7, 126.8, 125.4, 124.9, 124.5, 121.9, 120.2, 120.1, 117.4, 115.1, 112.9, 108.0, 70.3, 70.3, 70.0, 69.2, 68.2, 48.6, 41.9, 41.4, 19.4; **HR-ESI-MS** (*m/z*): calcd. for $C_{33}H_{33}N_6O_6$ $[M+H]^+$, 609.2456, found 609.2457.

4.1.4.2. 3-(((2-(2-(2-((Rutaecarpin-3-yl)oxy)ethoxy)ethoxy)ethyl)amino)methyl)-4-(3-fluro-phenyl)-1,2,5-oxadiazole-2-oxide (**13c**)

Yield: 56%, yellow solid. **^{1}H-NMR** (500 MHz, DMSO-d_6): δ 11.82 (s, 1H), 7.89 – 7.83 (m, 1H), 7.79 (d, *J* = 7.8 Hz, 1H), 7.66 – 7.59 (m, 3H), 7.53 (d, *J* = 2.9 Hz, 1H), 7.48 (d, *J* = 8.2 Hz, 1H), 7.46 (d, *J* = 2.5 Hz, 1H), 7.40 (dd, *J* = 8.9, 3.0 Hz, 1H), 7.29 – 7.23 (m, 1H), 7.09 (t, *J* = 7.5 Hz, 1H), 4.45 (t, *J* = 6.8 Hz, 2H), 4.20 – 4.15 (m, 2H), 3.82 (s, 2H), 3.79 – 3.74 (m, 2H), 3.58 (dd, *J* = 5.9, 3.5 Hz, 2H), 3.51 (dd, *J* = 5.8, 3.5 Hz, 2H), 3.45 (t, *J* = 5.4 Hz, 2H), 3.17 (t, *J* = 6.8 Hz, 2H), 2.67 (t, *J* = 5.5 Hz, 2H); **^{13}C-NMR** (126 MHz, DMSO-d_6): δ 160.8, 157.0, 143.8, 142.2, 139.0, 131.9, 131.8, 128.6, 127.7, 125.4, 124.9, 124.5, 124.5, 121.9, 120.2, 120.1, 118.6, 118.4, 117.4, 115.5, 115.3, 115.0, 113.0, 108.0, 70.4, 70.1, 69.3, 68.2, 48.6, 41.9, 41.4, 19.4; **HR-ESI-MS** (*m/z*): calcd. for $C_{33}H_{32}FN_6O_6$ $[M+H]^+$, 627.2362, found 627.2366.

4.1.4.3. 3-(((2-(2-(2-((Rutaecarpin-3-yl)oxy)ethoxy)ethoxy)ethyl)amino)methyl)-4-(2-ethoxy-phenyl)-1,2,5-oxadiazole-2-oxide (**13d**)

Yield: 67%, yellow solid. **^{1}H-NMR** (500 MHz, DMSO-d_6): δ 11.82 (s, 1H), 7.62 (dd, *J* = 8.4, 2.9 Hz, 2H), 7.58 – 7.53 (m, 2H), 7.53 – 7.46 (m, 2H), 7.41 (dd, J = 8.9, 2.9 Hz, 1H), 7.25 (t, *J* = 7.6 Hz, 1H), 7.19 (d, *J* = 8.4 Hz, 1H), 7.09 (q, *J* = 7.6 Hz, 2H), 4.45 (t, *J* = 6.8 Hz, 2H), 4.22 – 4.15 (m, 2H), 4.11 (q, *J* = 6.9 Hz, 2H), 3.78 –

3.73 (m, 2H), 3.71 (s, 2H), 3.55 – 3.49 (m, 2H), 3.42 (s, 2H), 3.29 (t, *J* = 5.4 Hz, 2H), 3.16 (t, *J* = 6.8 Hz, 2H), 2.48 (d, *J* = 5.4 Hz, 2H), 1.27 (t, *J* = 7.0 Hz, 3H). **^{13}C-NMR** (126 MHz, DMSO-d_6): δ 160.8, 157.0, 156.6, 156.5, 143.8, 142.2, 139.0, 133.4, 131.1, 130.0, 128.7, 127.7, 125.4, 124.9, 124.6, 121.9, 121.2, 120.2, 120.1, 117.4, 116.0, 115.3, 113.0, 108.0, 70.3, 70.1, 70.0, 69.3, 68.2, 64.4, 48.3, 41.9, 41.4, 19.4, 14.8. **HR-ESI-MS** (*m/z*): calcd. for $C_{35}H_{37}N_6O_7$ $[M+H]^+$, 653.2718, found 653.2730.

4.1.4.4. 3-(((2-(2-(2-((Rutaecarpin-3-yl)oxy)ethoxy)ethoxy)ethyl)amino)methyl)-4-(4-isopropyl-phenyl)-1,2,5-oxadiazole-2-oxide (**13e**)

Yield: 61%, yellow solid. **^{1}H-NMR** (500 MHz, DMSO-d_6): δ 11.83 (s, 1H), 7.85 (d, *J* = 8.3 Hz, 2H), 7.63 (dd, *J* = 11.7, 8.5 Hz, 2H), 7.55 (d, *J* = 3.0 Hz, 1H), 7.48 (d, *J* = 8.3 Hz, 1H), 7.45 – 7.39 (m, 3H), 7.28 – 7.23 (m, 1H), 7.09 (dd, *J* = 11.4, 4.2 Hz, 1H), 4.45 (t, *J* = 6.8 Hz, 2H), 4.24 – 4.14 (m, 2H), 3.81 (s, 2H), 3.79 – 3.74 (m, 2H), 3.58 (dd, *J* = 5.9, 3.5 Hz, 2H), 3.51 (dd, *J* = 5.7, 3.6 Hz, 2H), 3.45 (t, *J* = 5.4 Hz, 2H), 3.16 (t, *J* = 6.8 Hz, 2H), 2.98 – 2.91 (m, 1H), 2.67 (t, *J* = 5.4 Hz, 2H), 1.21 (d, *J* = 6.9 Hz, 6H); **^{13}C-NMR** (126 MHz, $CDCl_3$): δ 161.4, 157.2, 157.1, 152.3, 143.6, 141.7, 138.4, 127.8, 127.7, 127.4, 126.7, 125.4, 125.3, 125.0, 123.9, 121.5, 120.4, 119.9, 118.0, 114.4, 112.2, 107.7, 70.7, 70.3, 70.1, 69.5, 67.9, 48.3, 41.3, 34.1, 29.6, 23.7, 19.6; **HR-ESI-MS** (*m/z*): calcd. for $C_{36}H_{39}N_6O_6$ $[M+H]^+$, 651.2926, found 651.2925.

4.1.4.5. 3-(((2-(2-(2-((Rutaecarpin-3-yl)oxy)ethoxy)ethoxy)ethyl)amino)methyl)-4-(naphtha-1-yl)-1,2,5-oxadiazole-2-oxide (**13f**)

Yield: 57%, yellow solid. **^{1}H-NMR** (500 MHz, DMSO-d_6): δ 11.83 (s, 1H), 8.17 (t, *J* = 7.8 Hz, 1H), 8.09 – 8.01 (m, 2H), 7.89 (dt, *J* = 5.9, 2.9 Hz, 1H), 7.68 (dt, *J* = 13.5, 6.7 Hz, 1H), 7.66 – 7.60 (m, 4H), 7.55 (d, *J* = 2.9 Hz, 1H), 7.48 (d, *J* = 8.3 Hz, 1H), 7.43 – 7.39 (m, 1H), 7.25 (dd, *J* = 11.7, 4.5 Hz, 1H), 7.09 (t, *J* = 7.5 Hz, 1H), 4.45 (t, *J* = 6.8 Hz, 2H), 4.20 – 4.12 (m, 2H), 3.74 – 3.69 (m, 2H), 3.67 (s, 2H), 3.49 – 3.44 (m, 2H), 3.35 – 3.33 (m, 2H), 3.22 (dd, *J* = 13.3, 7.8 Hz, 2H), 3.17 (t, *J* = 6.8 Hz, 2H), 2.47 (t, *J* = 5.3 Hz, 2H); **^{13}C-NMR** (126 MHz, $CDCl_3$): δ 161.3, 157.2, 156.7, 143.3, 141.9, 138.3, 133.7, 131.5, 130.9, 128.78, 128.6, 128.0, 127.7, 127.1, 126.9, 125.6, 125.3, 125.2, 125.0, 124.4, 123.3, 121.7, 120.5, 119.9, 117.7, 115.3, 112.1, 107.7, 70.7, 70.3, 70.3, 69.6, 67.9, 48.3, 41.4, 41.3, 19.7; **HR-ESI-MS** (*m/z*): calcd. for

$C_{37}H_{35}N_6O_6$ $[M+H]^+$, 659.2613, found 659.2612.

4.1.4.6. 3-(((2-(2-(2-((Rutaecarpin-3-yl)oxy)ethoxy)ethoxy)ethyl)amino)methyl)-4-(fur -3-yl) -1,2,5-oxadiazole-2-oxide (**13g**)

Yield: 55%, brown solid. **^{1}H-NMR** (500 MHz, $CDCl_3$): δ 10.02 (s, 1H), 7.65 (d, *J* = 14.6 Hz, 2H), 7.58 (dd, *J* = 30.1, 8.4 Hz, 2H), 7.29 (q, *J* = 7.7 Hz, 3H), 7.15 (t, *J* = 5.9 Hz, 2H), 6.58 (s, 1H), 4.58 (t, *J* = 6.6 Hz, 2H), 4.21 (s, 2H), 4.05 (s, 2H), 3.87 (s, 2H), 3.71 (t, *J* = 3.1 Hz, 2H), 3.64 (t, *J* = 3.3 Hz, 2H), 3.62 – 3.57 (m, 2H), 3.21 (t, *J* = 6.6 Hz, 2H), 2.84 (t, *J* = 4.3 Hz, 2H); **^{13}C-NMR** (126 MHz, $CDCl_3$) δ 161.3, 157.2, 148.7, 145.2, 143.4, 142.0, 141.4, 138.3, 128.0, 127.2, 125.6, 125.3, 124.8, 121.7, 120.5, 119.9, 117.7, 112.9, 112.7, 112.1, 112.1, 107.7, 70.7, 70.4, 70.1, 69.6, 68.0, 48.3, 41.6, 41.3, 19.6; **HR-ESI-MS** (*m/z*): calcd. for $C_{31}H_{31}N_6O_7$ $[M+H]^+$, 599.2249, found 599.2248.

4.1.4.7. 3-(((2-(2-(2-((Rutaecarpin-3-yl)oxy)ethoxy)ethoxy)ethyl)amino)methyl)-4-(thiophen-3-yl)-1,2,5-oxadiazole-2-oxide (**13h**)

Yield: 66%, yellow solid. **^{1}H-NMR** (500 MHz, DMSO-d_6): δ 11.81 (s, 1H), 7.94 (dd, *J* = 3.7, 1.0 Hz, 1H), 7.89 (dd, *J* = 5.0, 0.9 Hz, 1H), 7.63 (d, *J* = 8.1 Hz, 1H), 7.61 (d, *J* = 8.9 Hz, 1H), 7.54 (d, *J* = 2.9 Hz, 1H), 7.48 (d, *J* = 8.3 Hz, 1H), 7.40 (dd, *J* = 8.9, 3.0 Hz, 1H), 7.28 (dd, *J* = 5.0, 3.8 Hz, 1H), 7.25 (d, *J* = 7.2 Hz, 1H), 7.09 (t, *J* = 7.5 Hz, 1H), 4.45 (t, *J* = 6.8 Hz, 2H), 4.24 – 4.15 (m, 2H), 3.87 (s, 2H), 3.81 – 3.75 (m, 2H), 3.60 (dd, *J* = 5.9, 3.5 Hz, 2H), 3.53 (dd, *J* = 5.7, 3.6 Hz, 2H), 3.47 (t, *J* = 5.4 Hz, 2H), 3.16 (t, *J* = 6.8 Hz, 2H), 2.70 (t, *J* = 5.5 Hz, 2H); **^{13}C-NMR** (126 MHz, DMSO-d_6): δ 160.8, 157.0, 153.0, 143.8, 142.2, 139.0, 131.5, 130.8, 128.9, 128.6, 127.7, 127.2, 125.4, 124.9, 124.5, 121.9, 120.2, 120.1, 117.4, 114.3, 112.9, 108.0, 70.3, 70.2, 70.1, 69.3, 68.2, 48.7, 41.9, 41.4, 19.4; **HR-ESI-MS** (*m/z*): calcd. for $C_{31}H_{31}N_6O_6S$ $[M+H]^+$, 615.2020, found 615.2020.

3-(((2-(2-((5-oxo-5,7,8,13-tetrahy-droindolo[2',3':3,4]pyrido[2,1-b]quinazolin-3-yl) oxy)ethoxy)ethyl)amino)methyl)-4-phenyl-1,2,5-oxadiazole 2-oxide (**13i**).

Yield: 43 %, yellow solid. ^{1}H-NMR (500 MHz, $CDCl_3$): δ 9.72 (s, 1H), 7.86 (d, *J* = 7.1 Hz, 2H), 7.69 (d, *J* = 1.9 Hz, 1H), 7.64 (d, *J* = 7.7 Hz, 2H), 7.53 (t, *J* = 6.7 Hz, 3H), 7.41 (d, *J* = 8.2 Hz, 1H), 7.33 (t, *J* = 7.6 Hz, 2H), 7.19 (t, *J* = 7.4 Hz, 1H), 4.58 (t,

J = 6.8 Hz, 2H), 4.22 (m, 2H), 3.99 (s, 2H), 3.86 (m, 2H), 3.74 – 3.69 (m, 2H), 3.24 (t, *J* = 6.8 Hz, 2H), 2.91 (m, 2H); ^{13}C-NMR (126 MHz, $CDCl_3$): δ 161.1, 157.3, 157.1, 143.3, 138.4, 131.1, 129.3, 128.0, 127.9, 127.7, 126.6, 125.6, 125.5, 125.1, 121.5, 120.7, 120.0, 113.9, 112.2, 107.8, 70.2, 69.5, 67.9, 48.5, 41.5, 41.3, 19.7. **HR-ESI-MS** (*m/z*): calcd. For $C_{31}H_{29}N_6O_5$ $[M+H]^+$, 565.2194, found 565.2207.

4.1.5. Procedures for the preparation of 3-(((2-(2-(2-((Rutaecarpin-10-yl)oxy) ethoxy)ethoxy) ethyl)amino)methyl)-4-phenyl-1,2,5-oxadiazole-2-oxide (**16**).

Step 1: To a solution of **14** (606 mg, 2.0 mmol) in DMF (5 mL) were added Cs_2CO_3 (975 mg, 3.0 mmol) and **11** (350 mg, 2.0 mmol) successively. The mixture was stirred at 60 °C for 4 hrs until no starting material was detected by TLC. The mixture was cooled to room temperature and was quenched with water, which was then extracted with EtOAc (50 mL × 3). The combined organic layer was washed with brine and was dried over Na_2SO_4, filtered, and concentrated in vacuum. The residue was purified by flash column chromatography (DCM : MeOH = 100 :1) to afford **15** as a yellow solid (148 mg, 16 %).

Step 2: To a solution of **15** (148 mg, 0.32 mmol) in MeOH (5.0 mL) was added Pd/C (15 mg, 10 %wt). The mixture was stirred at room temperature vigorously under hydrogen until no starting material was detected by TLC. Then the resulting suspension was filtered and the filtrate was concentrated in vacuum. The crude product was utilized for next step without further purification.

To a solution of the crude product in CH_3CN (3.0 mL) the solution was stirred at 60 °C after **9a** (86 mg, 0.32 mmol) and K_2CO_3 (0.5 mmol) was added. Upon there was no starting material was detected by TLC, the water was added to quench the reaction. The mixture then was extracted with EtOAc (50 mL × 3). The combined organic layer was washed with brine and was dried over Na_2SO_4, filtered, and concentrated in vacuum. The residue was purified by flash column chromatography (DCM : MeOH = 150 : 1) to afford **16** as a yellow solid (66 mg, 34 %). **^{1}H NMR** (400 MHz, $CDCl_3$): δ 9.49 (s, 1H), 8.33 (dt, *J* = 7.8, 2.0 Hz, 1H), 7.85 (dt, *J* = 5.6, 2.4 Hz, 2H), 7.76 – 7.69 (m, 1H), 7.66 (d, *J* = 7.6 Hz, 1H), 7.55 – 7.48 (m, 4H), 7.43 (ddd, *J* = 8.5, 7.5, 3.2 Hz, 2H), 7.26 – 7.21 (m, 1H), 7.01 (s, 1H), 4.58 (t, *J* = 6.9 Hz, 2H), 4.18 (t, *J* = 9.6, 4.7 Hz,

2H), 3.93 – 3.88 (m, 4H), 3.75 (m, *J* = 5.8, 3.2 Hz, 2H), 3.70 – 3.65 (m, 2H), 3.65 – 3.61 (m, 2H), 3.18 (t, *J* = 6.9 Hz, 2H), 2.86 – 2.80 (m, 2H); **^{13}C NMR** (101 MHz, $CDCl_3$): δ 161.6, 157.1, 153.7, 147.4, 145.1, 134.4, 133.8, 131.1, 129.2, 127.9, 127.5, 127.2, 126.6, 126.4, 126.2, 125.7, 121.0, 118.0, 117.2, 114.3, 113.0, 101.9, 70.7, 70.4, 70.2, 69.9, 68.1, 48.5, 41.6, 41.2, 19.7; **HR-ESI-MS** (*m/z*): calcd. for $C_{33}H_{33}N_6O_6$ $[M+H]^+$, 609.2456, found 609.2468.

4.1.6. Procedures for the preparation of 3-(((2-(2-(2-((Rutaecarpin-13-yl)oxy)ethoxy) ethoxy)ethyl)amino)methyl)-4-phenyl-1,2,5-oxadiazole-2-oxide (**18**)

Step 1: To a solution of **5c** (287 mg, 1.0 mmol) in CH_3CN (5.0 mL) were added compound **11** (175 mg, 1.0 mmol) and NaOH (80 mg, 2.0 mmol), the resulting mixture was stirred at 60 °C overnight. Then The reaction was quenched with water and was extracted with EtOAc (50 mL × 3). The combined organic layer was washed with brine and was dried over Na_2SO_4, filtered, and concentrated in vacuum. The residue was purified by flash column chromatography (pure DCM eluted) to afford **17** as a yellow solid (289 mg, 65 %).

Step 2: To a solution of compound **17** (222mg, 0.5 mmol) in MeOH (5.0 mL) was added Pd/C (22 mg, 10 %wt) in one portion. The mixture was stirred vigorously at room temperature under hydrogen until no starting material was detected by TLC. Then the suspension was filtered and the filtrate was concentrated in vacuum. The residue was dissolved in CH_3CN (2.5 mL). And then **9a** (135 mg, 0.5 mmol) and K_2CO_3 (104 mg, 0.75 mmol) were added successively. The resulting mixture was stirred at 60 °C until no starting material was detected by TLC. Then the reaction was quenched with water and was extracted with EtOAc (50 mL × 3). The combined organic layer was washed with brine and was dried over Na_2SO_4, filtered, and concentrated in vacuum. The residue was purified by flash column chromatography (pure DCM) to afford **18** as a yellow solid (130 mg, 44 %). **^{1}H-NMR** (500 MHz, $CDCl_3$): δ 8.35 – 8.29 (m, 1H), 7.83 (dd, *J* = 7.4, 2.0 Hz, 2H), 7.75 – 7.70 (m, 1H), 7.67 – 7.63 (m, 1H), 7.60 (d, *J* = 8.0 Hz, 1H), 7.58 – 7.54 (m, 1H), 7.53 – 7.48 (m, 3H), 7.43 (dd, *J* = 13.1, 6.0 Hz, 1H), 7.36 (t, *J* = 7.5 Hz, 1H), 7.17 (t, *J* = 7.5 Hz, 1H), 5.03 (t, *J* = 5.9 Hz, 2H), 4.54 (dd, *J* = 12.4, 5.7 Hz, 2H), 4.04 – 3.99 (m, 2H), 3.82 (d,

J = 7.4 Hz, 2H), 3.62 – 3.57 (m, 2H), 3.54 – 3.50 (m, 2H), 3.47 (t, *J* = 5.0 Hz, 2H), 3.16 (t, *J* = 6.7 Hz, 2H), 2.72 (t, *J* = 5.0 Hz, 2H); **^{13}C-NMR** (126 MHz, $CDCl_3$): δ 161.7, 157.1, 147.3, 145.3, 140.6, 134.1, 131.1, 129.2, 127.9, 127.1, 127.0, 126.7, 126.6, 126.3, 125.2, 124.1, 120.8, 120.4, 119.9, 119.5, 114.1, 111.1, 71.0, 70.8, 70.4, 70.1, 48.5, 45.0, 41.4, 40.8, 19.7; **HR-ESI-MS** (*m/z*): calcd. for $C_{33}H_{33}N_6O_5$ $[M+H]^+$, 593.2507, found 593.2530.

4.2. Biology methods

All animals received humane care in compliance with Guide for the Care and Use of Laboratory Animals published by the National Institutes of Health. Capsazepine, phenylepherine, HC030031 were purchased from Selleck Chemicals company, and CGRP-(8-37) and dimethyl sulfoxide from Sigma-Aldrich Chemical company. In the study of vasodilator effects, the candidate compounds, phenylepherine, HC030031, and capsazepine were initially dissolved in dimethyl sulfoxide, and further diluted in Kreb's solution to the proper final concentration. The final concentration of dimethyl sulfoxide did not exceed 0.1%, which had no effect on vascular tension. CGRP-(8-37) was dissolved in distilled water. In the case of the intra-arterial pressures measurement, candidate compounds was suspended at a sodium carboxymethyl cellulose solution.

4.2.1 Vasodilator responses assay

Male Sprague-Dawley rats (250-300 g) were anesthetized with 10% chloral hydrate (1.25 mL/kg, i.p.) and the thoracic aorta were rapidly isolated cleaned of fat and connective tissues, and then cut into rings of 4 mm length. The rings were suspended horizontally between two stainless steel wires and mounted in a 10mL-organ chamber filled with warmed (37 °C) and oxygenated (95% O_2 and 5% CO_2) Krebs' solution, which had the following composition (mM): NaCl, 119.0; $NaHCO_3$, 25.0; KCl, 4.7; KH_2PO_4, 1.2; $MgSO_4$, 1.2; $CaCl_2$, 2.5; and glucose, 11.0. Each of the rings' end was connected to a force transducer. The aortic rings were stretched with 2 g resting force, equilibrated for 60 min, and then pre-contracted with phenylephrine (60 mM, final concentration). After a maximal response to KCl was observed, the rings were washed with Krebs' solution and equilibrated for another 30 min, hereafter

incubated with cysteine (1μM, final concentration) for 10 minutes. The rings were contracted with phenylephrine (2 μM, final concentration). After the contraction had stabilized, a cumulative concentration–response curve to rutaecarpine and other candidates (10^{-9} – 10^{-6} M, final concentration) was observed.

4.2.2. The vasodilator effect was inhibited with HC030031, capsazepine or CGRP(8-37).

The thoracic aorta was prepared in the same way as mentioned in 4.2.1. After a maximal response to KCl was observed, the rings were washed with Krebs'solution and equilibrated for another 30 minutes, then the rings were divided randomly into five groups as follows: (1) control group, the rings were incubated with L-cysteine (1μM, final concentration) for 10 minutes; (2) HC030031 group, the rings were incubated with L-cysteine (1μM, final concentration) and HC030031 (10 μM, final concentration) for 10 minutes; (3) capsazepine group, the rings were incubated with L-cysteine (1μM, final concentration) and capsazepine (10 μM, final concentration) for 10 minutes; (4) HC030031-capsazepine group, the rings were incubated with L-cysteine (1μM, final concentration), HC030031 (10 μM, final concentration) and capsazepine (10 μM, final concentration) for 10 minutes; (5) CGRP(8-37) group, the rings were incubated with L-cysteine (1μM, final concentration) and CGRP(8-37) (10 μM, final concentration) for 10 minutes. After that the rings were contracted with phenylephrine (2 μM, final concentration). When the contraction stabilized, a cumulative concentration–response curve to candidates (10^{-9}–10^{-6} M, final concentration) was observed.

4.2.3 Intra-arterial pressures measured by carotid cannulation

Male Sprague-Dawley rats weighing 250-300 g were naesthetized with sodium pentobarbital, 40 mg/Kg body weight (b.wt.). Body temperature was maintained at 37ºC and a tracheotomy was performed. The right carotid artery was cannulated with PE-10 tubing connected to PE-50 tubing and to a pressure transducer. Arterial pressure (AP) was recorded by a digital data recorder (MacLab/4e, AD Instruments, Australia) and analyzed using Chart v 3.4 (an application program). The candidates were administered by intra-peritoneal injection when the intra-arterial pressures were

stable (low dose group: 20 mg/kg; high dose group: 40 mg/kg) and supplemental doses of anesthesia (sodium pentobarbital: 10 mg/Kg b. wt.) were administrated as required. Then the changes in arterial pressure within 2 hours were recorded continuously, and a histogram of decrease in arterial pressure was obtained.

4.2.4. ELISA analysis

The CGRP ELISA immunoassay kit (Huijia Biotech., China) was used to quantify the amount of rat CGRP present in the serum. The CGRP assay was performed according to the manufacturer's instructions. The optical density was measured at a wavelength of 450 nm using an ELISA microplate reader (PerkinElmer EnSpire). Concentrations were calculated and are expressed as pg/mL.

4.2.5. Statistical analysis

All statistical analyses were conducted using SPSS 19.0 software for Windows (Chicago, IL). Statistically significant differences were determined by two-way ANOVA, and P values less than 0.05 were considered statistically significant in all cases.

Acknowledgment. We thank Prof. Liu from the Instrumental Analysis Center of Central South University for NMR spectra analysis and Prof. Niansheng Li for kind help in pharmacological experiments. Financial support was provided by National Natural Science Foundation of China (21302193 and 81573314), Nature Science Foundation of Hunan Province (2018JJ3707), Changsha Science and Technology Projects (kq1701088), and the Start-up funds of Central South University (Xu Deng).

Appendix. Supplementary Information.

Supplementary information associated with this article can be found in the online version. These data include NMR spectrums of the most compounds described in this article.

Conflicts of interest.

The authors declare no competing financial interest.

References

[1] K.L. Ong, B.M.Y. Cheung, Y.B. Man, C.P. Lau, K.S.L. Lam, Prevalence, awareness, treatment, and control of hypertension among United States adults 1999-2004, Hypertension, 49 (2007) 69-75.

[2] F.F. Costa Filho, A. Timerman, J.F.K. Saraiva, C.C. Magalhaes, I.M.F. Pinto, G.B.F. Oliveira, A.C. Mattos, A. Avezum, Independent predictors of effective blood pressure control in patients with hypertension on drug treatment in Brazil, J. Clin. Hypertens. , 20 (2018) 125-132.

[3] D. Li, X.-J. Zhang, L. Chen, Z. Yang, H.-W. Deng, J. Peng, Y.-J. Li, Calcitonin gene-related peptide mediates the cardioprotective effects of rutaecarpine against ischemia-reperfusion injury in spontaneously hypertensive rats, Clin. Exp. Pharmacol. Physiol., 36 (2009) 662-667.

[4] F. Portaluppi, G. Trasforini, A. Margutti, L. Vergnani, M.R. Ambrosio, R. Rossi, B. Bagni, R. Pansini, U.E.C. degli, Circadian rhythm of calcitonin gene-related peptide in uncomplicated essential hypertension, J. Hypertens., 10 (1992) 1227-1234.

[5] Q.-Q. Chen, D. Li, R. Guo, D. Luo, J. Yang, C.-P. Hu, Y.-J. Li, Decrease in the synthesis and release of calcitonin gene-related peptide in dorsal root ganglia of spontaneously hypertensive rat: Role of nitric oxide synthase inhibitors, Eur. J. Pharmacol., 596 (2008) 132-137.

[6] W. Chai, S. Mehrotra, A.H.J. Danser, R.G. Schoemaker, The role of calcitonin gene-related peptide (CGRP) in ischemic preconditioning in isolated rat hearts, Eur. J. Pharmacol., 531 (2006) 246-253.

[7] J. Peng, Y.-J. Li, The vanilloid receptor TRPV1: Role in cardiovascular and gastrointestinal protection, Eur. J. Pharmacol., 627 (2010) 1-7.

[8] S.D. Brain, A.D. Grant, Vascular actions of calcitonin gene-related peptide and adrenomedullin, Physiol. Rev., 84 (2004) 903-934.

[9] Y. Wang, D.H. Wang, A novel mechanism contributing to development of Dahl salt-sensitive hypertension: role of the transient receptor potential vanilloid type 1, Hypertension, 47 (2006) 609-614.

[10] A.A. Aubdool, X. Kodji, N. Abdul-Kader, R. Heads, E.S. Fernandes, S. Bevan, S.D. Brain, TRPA1 activation leads to neurogenic vasodilatation: involvement of reactive oxygen nitrogen species in addition to CGRP and NO, Br. J. Pharmacol., 173 (2016) 2419-2433.

[11] G. Pozsgai, J.V. Bodkin, R. Graepel, S. Bevan, D.A. Andersson, S.D. Brain, Evidence for the pathophysiological relevance of TRPA1 receptors in the cardiovascular system in vivo, Cardiovasc. Res., 87 (2010) 760-768.

[12] T. Quallo, C. Gentry, S. Bevan, L.M. Broad, A.J. Mogg, Activation of transient receptor potential ankyrin 1 induces CGRP release from spinal cord synaptosomes, Pharmacol. Res. Perspect., 3 (2015) e00191.

[13] E.D.H. P. M. Zygmunt, Mammalian Transient Receptor Potential (TRP) Cation Channels, Springer, Berlin Heideberg, 2014.

[14] L.J. Macpherson, A.E. Dubin, M.J. Evans, F. Marr, P.G. Schultz, B.F. Cravatt, A. Patapoutian, Noxious compounds activate TRPA1 ion channels through covalent modification of cysteines, Nature, 445 (2007) 541-545.

[15] K. Alawi, J. Keeble, The paradoxical role of the transient receptor potential vanilloid 1 receptor in inflammation, Pharmacol. Ther., 125 (2010) 181-195.

[16] S. Jia, C. Hu, Pharmacological effects of rutaecarpine as a cardiovascular protective agent, Molecules, 15 (2010) 1873-1881.

[17] S.H. Lee, J.-K. Son, B.S. Jeong, T.-C. Jeong, H.W. Chang, E.-S. Lee, Y. Jahng, Progress in the studies on rutaecarpine, Molecules, 13 (2008) 272-300.

[18] J.-K. Son, H.W. Chang, Y. Jahng, Progress in Studies on Rutaecarpine. II.--Synthesis and

Structure-Biological Activity Relationships, Molecules, 20 (2015) 10800-10821.
[19] C.-P. Hu, L. Xiao, H.-W. Deng, Y.-J. Li, The depressor and vasodilator effects of rutaecarpine are mediated by calcitonin gene-related peptide, Planta Med., 69 (2003) 125-129.
[20] Y. Kobayashi, K. Hoshikuma, Y. Nakano, Y. Yokoo, T. Kamiya, The positive inotropic and chronotropic effects of evodiamine and rutaecarpine, indoloquinazoline alkaloids isolated from the fruits of Evodia rutaecarpa, on the guinea-pig isolated right atria: possible involvement of vanilloid receptors, Planta Med., 67 (2001) 244-248.
[21] C.-P. Hu, L. Xiao, H.-W. Deng, Y.-J. Li, The cardioprotection of rutaecarpine is mediated by endogenous calcitonin related-gene peptide through activation of vanilloid receptors in guinea-pig hearts, Planta Med., 68 (2002) 705-709.
[22] B. Wen, V. Roongta, L. Liu, D.J. Moore, Metabolic activation of the indoloquinazoline alkaloids evodiamine and rutaecarpine by human liver microsomes: dehydrogenation and inactivation of cytochrome P450 3A4, Drug Metab. Dispos., 42 (2014) 1044-1054.
[23] X.W. Yang, H. Zhang, M. Li, L.J. Du, Z. Yang, S.Y. Xiao, Studies on the alkaloid constituents of Evodia rutaecarpa (Juss) Benth var. bodinaieri (Dode) Huang and their acute toxicity in mice, J. Asian Nat. Prod. Res., 8 (2006) 697-703.
[24] Z. Chen, G. Hu, D. Li, J. Chen, Y. Li, H. Zhou, Y. Xie, Synthesis and vasodilator effects of rutaecarpine analogues which might be involved transient receptor potential vanilloid subfamily, member 1 (TRPV1), Bioorg. Med. Chem., 17 (2009) 2351-2359.
[25] J.S. Stamler, E. Loh, M.-A. Roddy, K.E. Currie, M.A. Creager, Nitric oxide regulates basal systemic and pulmonary vascular resistance in healthy humans, Circulation, 89 (1994) 2035-2040.
[26] N. Tuteja, M. Chandra, R. Tuteja, M.K. Misra, Nitric oxide as a unique bioactive signaling messenger in physiology and pathophysiology, J. Biomed. Biotechnol., (2004) 227-237.
[27] M. Eberhardt, M. Dux, B. Namer, J. Miljkovic, N. Cordasic, C. Will, T.I. Kichko, J. de la Roche, M. Fischer, S.A. Suarez, D. Bikiel, K. Dorsch, A. Leffler, A. Babes, A. Lampert, J.K. Lennerz, J. Jacobi, M.A. Marti, F. Doctorovich, E.D. Hoegestaett, P.M. Zygmunt, I. Ivanovic-Burmazovic, K. Messlinger, P. Reeh, M.R. Filipovic, H2S and NO cooperatively regulate vascular tone by activating a neuroendocrine HNO-TRPA1-CGRP signalling pathway, Nat. Commun., 5 (2014) 4381-4398.
[28] A.M.H. Pinkney, H.A.L. Lemmey, K.A. Dora, C.J. Garland, Vasorelaxation to the Nitroxyl Donor Isopropylamine NONOate in Resistance Arteries Does Not Require Perivascular Calcitonin Gene-Related Peptide, Hypertension, (2017).
[29] H. Nakagawa, Photocontrollable nitric oxide (NO) and nitroxyl (HNO) donors and their release mechanisms, Nitric Oxide, 25 (2011) 195-200.
[30] C. Medana, A. Di Stilo, S. Visentin, R. Fruttero, A. Gasco, D. Ghigo, A. Bosia, NO donor and biological properties of different benzofuroxans, Pharm. Res., 16 (1999) 956-960.
[31] Y. Yang, C. Zhu, M. Zhang, S. Huang, J. Lin, X. Pan, W. Su, Condensation of anthranilic acids with pyridines to furnish pyridoquinazolones via pyridine dearomatization, Chem. Comm., 52 (2016) 12869-12872.

Figure Captions

Figure 1. The chemical structure of rutaecarpine

Figure 2. Concentration–response curve of vasodilator effect to rat aortic rings. Value represent mean ± REM, n = 5, *P < 0.05 vs **Rut**, **p < 0.01 vs **Rut**, $^{+}$p < 0.05 vs **Rut**+Furoxan group).

Figure 3. Concentration–response curve of vasodilator effect of **13a** to rat aortic rings. Capsaicin was exposed for 20 min, and then was washed with fresh Krebs' solution. CGRP-(8-37) or capsazepine was exposed for 10 min before vasodilator response to **13a** (value represent mean ± REM, n = 5, *P < 0.05, **P < 0.01 *vs* **13a**).

Figure 4. Effect of **13a** on blood pressure (value represent mean ± REM, n = 5, *P < 0.05, **P < 0.01 *vs* **Rut**).

Scheme 1. Synthesis of rutaecarpine derivatives. Reagents and conditions: (i) ethyl formate, reflux, 100%; (ii) $POCl_3$, DCM, 0 °C; (iii) EDCI, DMF, air, 80 °C;

Scheme 2. Synthesis of rutaecarpine-furoxan hybrids tethered at 3-position. Reagents and conditions: (i) Malonic acid, piperidine, DMF, 80 °C; (ii) BH_3-THF (1 M in THF), 0 °C to R.T.; (iii) $NaNO_2$ (aq.), AcOH, 0 °C to R.T.; (iv) MsCl, TEA, DCM, 0 °C to R.T.; (v) step 1: MsCl, TEA, DCM, 0 °C to R.T.; step 2: NaN_3, ethanol, reflux; (vi) MsCl, TEA, DCM, 0 °C to R.T.; (vii) K_2CO_3, DMF, 80 °C; (viii) H_2, Pd/C, MeOH, R.T.; (ix) **9a-9g**, K_2CO_3, CH_3CN, 60 °C;

Scheme 3. Synthesis of rutaecarpine-furoxan hybrids tethered at 10- and 13-position. Reagents and conditions: (i) BBr_3, DCM, -78 °C-0 °C; (ii) NaOH, CH_3CN, 70 °C; (iii) step 1: H_2, Pd/C, MeOH, R.T.; step 2: **9a**, K_2CO_3, CH_3CN, 60 °C;

Table 1. The vasodilator effects of rutaecarpine and rutaecarpine-furoxan hybrids

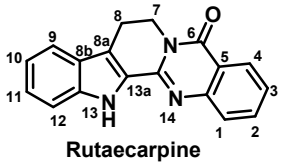

Figure 1. The chemical structure of rutaecarpine

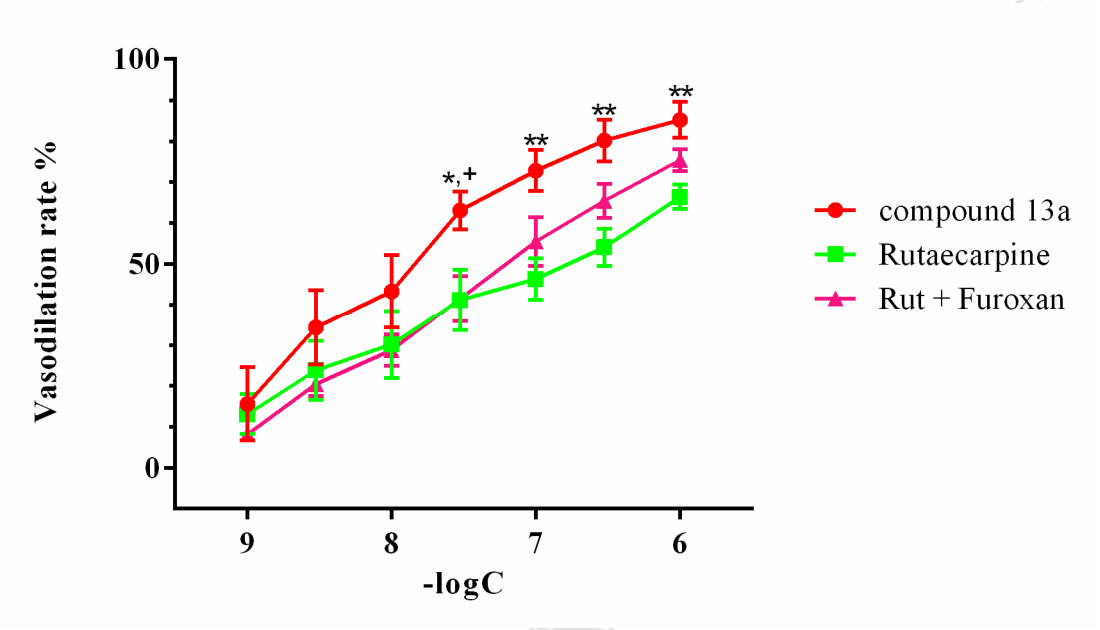

Figure 2. Concentration–response curve of vasodilator effect to rat aortic rings. Value represent mean ± REM, n = 5, *P < 0.05 vs **Rut**, **p < 0.01 vs **Rut**, $^{+}$p < 0.05 vs **Rut**+Furoxan group).

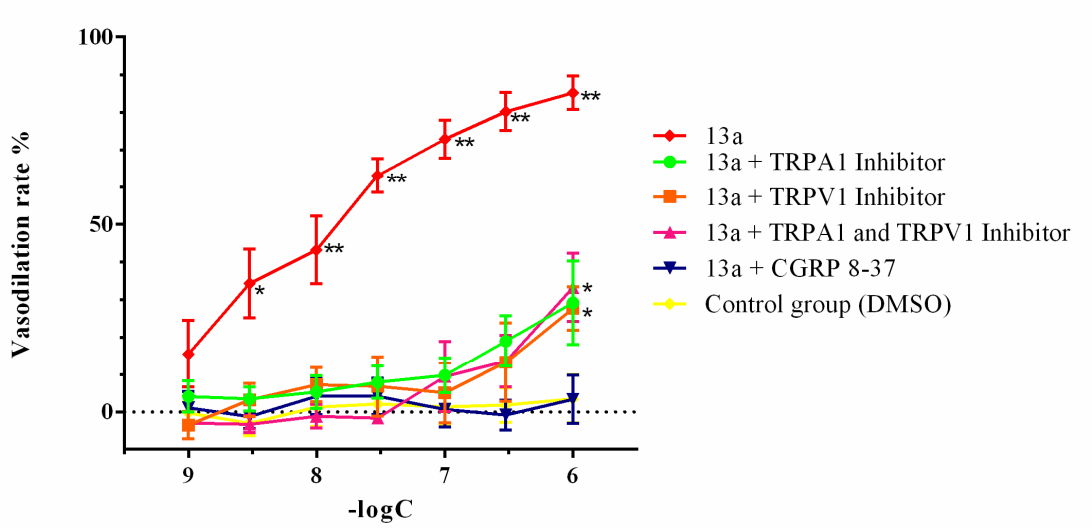

Figure 3. Concentration–response curve of vasodilator effect of **13a** to rat aortic rings.

Capsaicin was exposed for 20 min, and then was washed with fresh Krebs' solution. CGRP-(8-37) or capsazepine was exposed for 10 min before vasodilator response to **13a** (value represent mean ± REM, n = 5, *P < 0.05, **P < 0.01 *vs* **13a**).

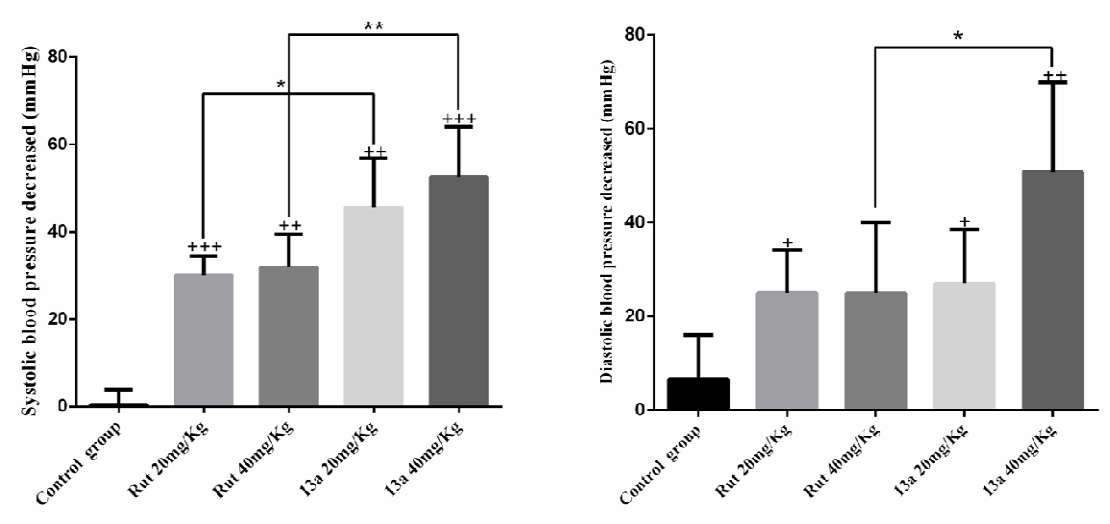

Figure 4. Effect of **13a** on blood pressure (value represent mean ± REM, n = 5, *P < 0.05, **P < 0.01 *vs* **Rut**).

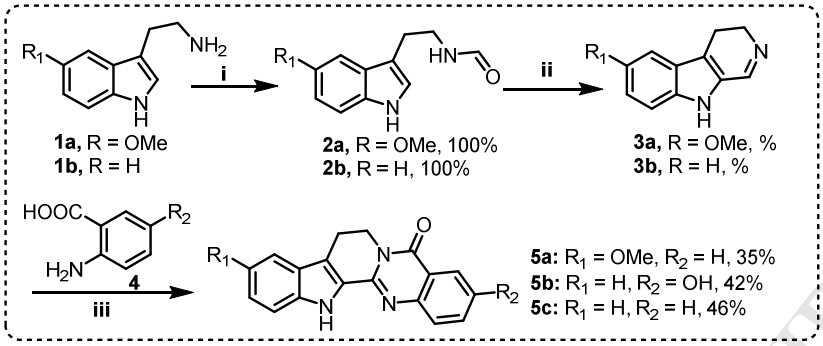

Scheme 1. Synthesis of rutaecarpine derivatives. Reagents and conditions: (i) ethyl formate, reflux, 100%; (ii) $POCl_3$, DCM, 0 °C; (iii) EDCI, DMF, air, 80 °C;

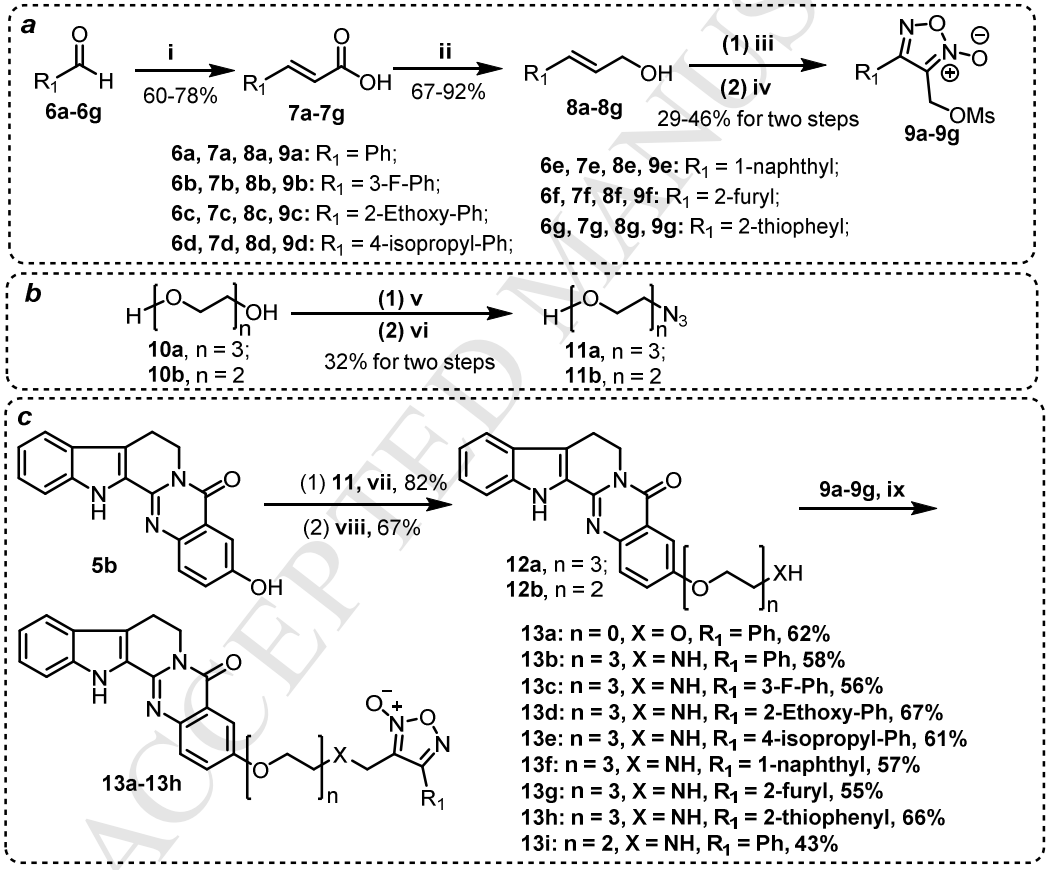

Scheme 2. Synthesis of rutaecarpine-furoxan hybrids tethered at 3-position. Reagents and conditions: (i) Malonic acid, piperidine, DMF, 80 °C; (ii) BH_3-THF (1 M in THF), 0 °C to R.T.; (iii) $NaNO_2$ (aq.), AcOH, 0 °C to R.T.; (iv) MsCl, TEA, DCM, 0 °C to R.T.; (v) step 1: MsCl, TEA, DCM, 0 °C to R.T.; step 2: NaN_3, ethanol, reflux; (vi) MsCl, TEA, DCM, 0 °C to R.T.; (vii) K_2CO_3, DMF, 80 °C; (viii) H_2, Pd/C, MeOH, R.T.; (ix) **9a-9g**, K_2CO_3, CH_3CN, 60 °C;

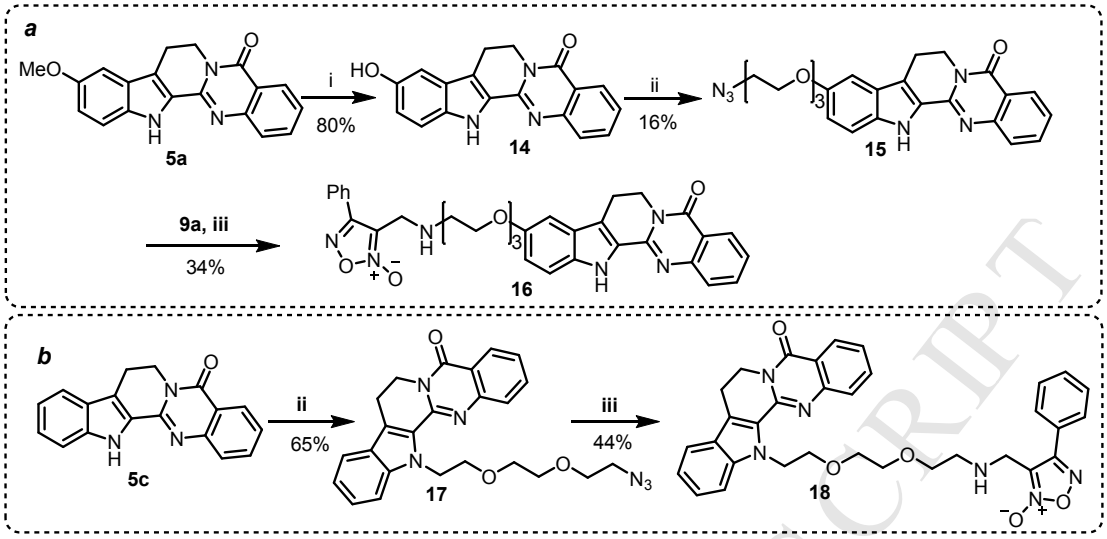

Scheme 3. Synthesis of rutaecarpine-furoxan hybrids tethered at 10- and 13-position. Reagents and conditions: (i) BBr_3, DCM, -78 °C-0 °C; (ii) NaOH, CH_3CN, 70 °C; (iii) step 1: H_2, Pd/C, MeOH, R.T.; step 2: **9a**, K_2CO_3, CH_3CN, 60 °C;

Table 1. The vasodilator effects of rutaecarpine and rutaecarpine-furoxan hybrids

Entry	EC50 (mol/L)	E_{max} ± SD (%)
13a	1.31×10^{-8}**	85.2 ± 9.9
13b	7.74×10^{-7}	54.6 ± 14.7
13c	1.58×10^{-7}	77.3 ± 10.6
13d	1.16×10^{-7}	69.9 ± 12.3
13e	2.59×10^{-6}*	40.9 ± 14.0
13f	1.41×10^{-6}*	45.3 ± 14.8
13g	2.25×10^{-5}***	30.6 ± 9.2
13h	3.07×10^{-8}	73.6 ± 10.2
13i	1.52×10^{-8}	81.4 ± 11.0
16	1.12×10^{-7}	64.2 ± 8.0
18	2.04×10^{-6}	43.2 ± 21.4
Rut	1.56×10^{-7}	66.3 ± 6.6
Rut+Furoxan	2.97×10^{-8}	75.3 ± 5.8

[a]E_{max} ± REM (%), n = 5, *P<0.5, **P<0.01, ***P<0.001 versus rutaecarpine.

Highlights

Dual-targeting Rutaecarpine-NO Donor Hybrids as Novel Anti-hypertensive Agents by Promoting Release of CGRP

Jinjin Ma,[†,1] Lan Chen,[†,1] Jinbao Fan,[†] Wei Cao,[†] Guangyao Zeng,[†] Yajing Wang,[‡] Yuanjian Li,[†] Yingjun Zhou,[*,†] Xu Deng[*,†]

1. Regulating the release of CGRP represents a new approach for anti-hypertensive drug discovery.
2. Hybridization strategy by dually targeting TRPV1 and TRPA1 was applied.
3. Rutaecarpine and furoxan-type NO donors are promising active phamacophores.
4. **13a** exhibited significantly improved *ex-vivo* (EC_{50} = 13.1 nM) and *in-vivo* activity.